GEOPHYSICS, VOL. 77, NO. 5 (SEPTEMBER-OCTOBER 2012); P. WC163–WC171, 11 FIGS.
10.1190/GEO2012-0133.1

Application of 3D seismic techniques to evaluate ore resources in the West Wits Line goldfield and portions of the West Rand goldfield, South Africa

Musa S. D. Manzi[1], Mark A. S. Gibson[2], Kim A. A. Hein[1], Nick King[3], and Raymond J. Durrheim[4]

ABSTRACT

As expensive as 3D seismic reflection surveys are, their high cost is justified by improved imaging of certain ore horizons in some of the Witwatersrand basin gold mines. The merged historical 3D seismic reflection data acquired for Kloof and South Deep mines forms an integral part of their Ventersdorp Contact Reef mine planning and development programme. The recent advances in 3D seismic technology have motivated the reprocessing and reinterpretation of the old data sets using the latest algorithms, therefore significantly increasing the signal-to-noise ratio of the data. In particular, the prestack time migration technique has provided better stratigraphic and structural imaging in complex faulted areas, such as the Witwatersrand basin, relative to older poststack migration methods. Interpretation tools such as seismic attributes have been used to identify a number of subtle geologic structures that have direct impact on ore resource evaluation. Other improvements include more accurate mapping of the depths, dip, and strike of the key seismic horizons and auriferous reefs, yielding a better understanding of the interrelationship between fault activity and reef distribution, and the relative chronology of tectonic events. The 3D seismic data, when integrated with underground mapping and borehole data, provide better imaging and modeling of critical major fault systems and zones of reef loss. Many faults resolve as multifault segments that bound unmined blocks leading to the discovery and delineation of resources in faulted areas of the mines.

INTRODUCTION

In the early 1980s, the planning of new mines and extension of existing mines relied mostly on geologic models that were based on a combination of gravity, aeromagnetic, and borehole data (Durrheim, 1986; Stevenson et al., 2003). Although magnetic and gravity techniques are effective in the delineation of subsurface structures such as dikes and major faults (Weder, 1994; Trickett et al., 2004), they are unable to map the structure of deeply buried strata in detail (Pretorius et al., 1994; Stevenson et al., 2003), which is critical for the very deep gold mines of the Witwatersrand Basin. Furthermore, they cannot resolve gold-bearing reefs and fault geometries with the accuracy required for optimal mine planning (Stevenson et al., 2003; Trickett et al., 2004). Although borehole data provide accurate geologic information, this information is restricted to the vicinity of the borehole (Trickett et al., 2004).

Since the late 1980s, the Witwatersrand gold mines have made use of 3D seismic reflection surveys to facilitate reliable mine planning and design. In 2003, Gold Fields Ltd. conducted a high-resolution 3D seismic reflection survey (the Kloof-South Deep survey), targeting the down-dip portion of the auriferous Ventersdorp Contact Reef (VCR) in the Kloof and South Deep gold mines, which are located west and east of the West Rand Fault, respectively (Figure 1). The Kloof gold mine is a large, shallow to ultradeep level mine with workings accessed through five shaft systems. The mine exploits various gold reefs (mainly VCR) at depths

Manuscript received by the Editor 16 April 2012; published online 6 September 2012.
[1]University of the Witwatersrand, School of Geosciences, Johannesburg, Republic of South Africa. E-mail: musa.manzi@students.wits.ac.za; kim.ncube-hein@wits.ac.za.
[2]High Power Exploration, Johannesburg, Republic of South Africa. E-mail: mark.g@ipulse.fr.
[3]Gold Fields Limited, South Deep Gold Mine, Johannesburg, Republic of South Africa. E-mail: nick.king@goldfields.co.za.
[4]University of the Witwatersrand, School of Geosciences, Johannesburg, Republic of South Africa and CSIR Center for Mining Innovation, Johannesburg, Republic of South Africa. E-mail: raymond.durrheim@wits.ac.za.
© 2012 Society of Exploration Geophysicists. All rights reserved.

Downloaded 09 Sep 2012 to 41.132.206.56. Redistribution subject to SEG license or copyright; see Terms of Use at http://segdl.org/

between 2000 and 3350 m below the surface. The South Deep gold mine is an intermediate to ultradeep level mine comprising two shaft systems. It exploits VCR and Upper Elsburg reefs at depths between 2000 and 3500 m below the surface. The primary objective of the survey was to image the VCR orebody to the northwest and southeast of the West Rand Fault over the depth range of 2000 to 4500 m. The true seismic volume extends to approximately 9 km deep, with an east–west extent of 40 km and north–south extent of 16 km (i.e., 5760 km^3). The secondary objective was to image the cutoff of the VCR on the downthrown and upthrown blocks of the West Rand Fault to assist resource evaluation and mine planning.

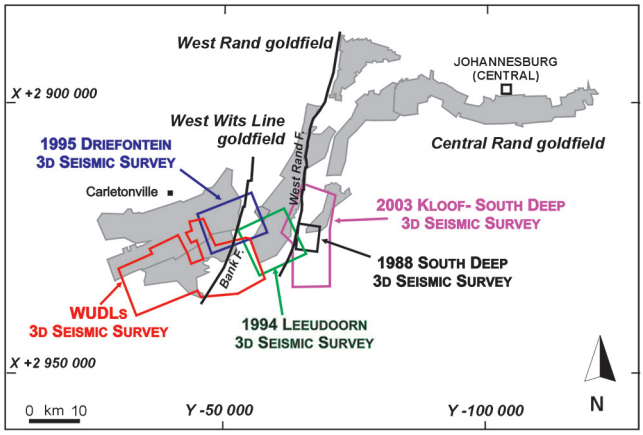

Figure 1. Location of the Witwatersrand basin historical 3D seismic reflection survey areas (after Gibson et al., 2000).

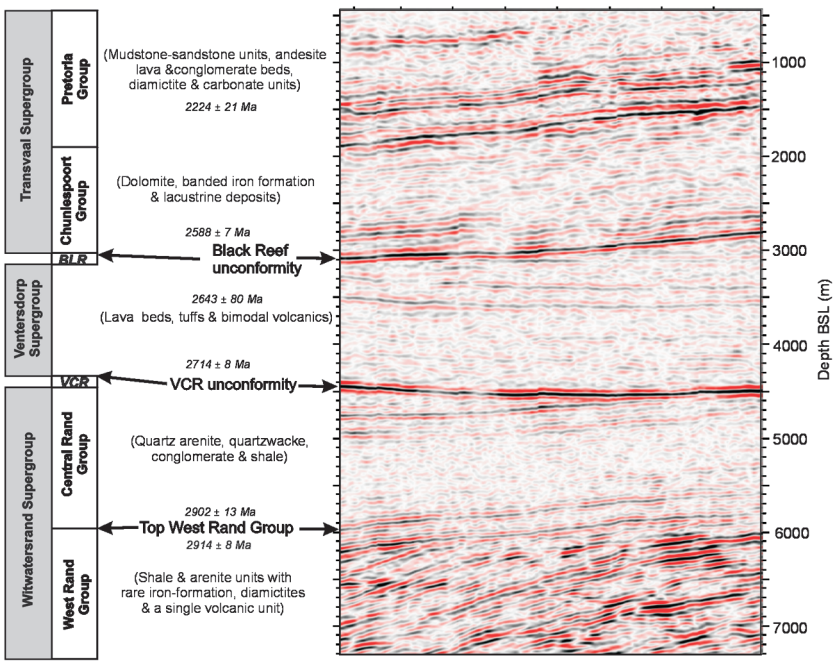

Figure 2. Generalized stratigraphy of the West Wits Line goldfield, derived from the depth-converted PSTM seismic section. Geochronological data and geology after Dankert and Hein (2010).

Recently, the application of 3D seismic imaging has brought precision to drilling boreholes in geologically complex areas (De Wet and Hall, 1994; Trickett et al., 2004). In this study, we present the detailed interpretation of five merged historical 3D seismic reflection surveys from gold mines on the West Wits Line and West Rand. We also show how the new migration algorithms and improvement in interpretation techniques can maximize the high-resolution image of ore horizons and structures, thus improving mine planning and design and reducing mining risks.

The 2003 Kloof-South Deep survey was designed to overlap with the 1988 South Deep survey, the first 3D seismic survey conducted in South Africa, and the 1994 Leeudoorn 3D seismic survey. The three surveys were merged and processed as a single entity of final depth-converted prestack time migrated (PSTM) seismic volume to produce a single seismic cube. To improve the resolution of the old data, the 1994 Leeudoorn data set was reprocessed using the latest processing algorithms. Following the successful interpretation of the data, the single seismic cube was merged (postmigration) with the Western Ultra Deep Levels (WUDLs) survey, which was acquired in 1995 and covers the Driefontein gold mine to the west of the Bank Fault (Figure 1). The Driefontein gold mine comprises eight shaft systems. It exploits various gold-bearing reefs, mainly VCR and Carbon Leader Reef (CLR) that occur at depths between 600 and 3300 m below the surface. The WUDLs survey also covers the Mponeng, Savuka, and Tautona gold mines. The Mponeng Mine is one of the deepest and richest gold mines in the world, exploiting VCR at depths between 2400 and 3900 m below the surface, whereas the Savuka and Tautona gold mines exploit mainly CLR at depths up to 3450 m.

These data sets were incorporated into one continuous volume and used to study the regional structural setting, including major and minor structures. The overall aims were to investigate (1) the application of the PSTM technique in structural enhancement, (2) the geometry of faults and their impact on mining, and (3) the use of attribute analysis to map structures that cannot be resolved through conventional interpretation.

GEOLOGIC SETTING AND MINEABLE REEFS

The famous Archean Witwatersrand basin is the largest gold province in the world (Phillips and Law, 2000; McCarthy, 2006). In the past century, it has produced about 40% of the world's mined gold and is estimated to still contain 30% of the world's known gold reserves (Stanistreet and McCarthy, 1991). Its exploration and exploitation has produced a huge geologic and geophysical database.

A generalized lithostratigraphic column of the Witwatersrand basin is summarized in Figure 2. The Witwatersrand Supergroup overlies the Dominion Group unconformably and comprises lower and upper successions, namely the West Rand and Central Rand Groups (Dankert and Hein, 2010). The Dominion Group is not shown on Figure 2 because it is beneath our zone of interest.

Downloaded 09 Sep 2012 to 41.132.206.56. Redistribution subject to SEG license or copyright; see Terms of Use at http://segdl.org/

The West Rand Group unconformably overlies the Dominion Group with clastic and largely marine sediments (ca. 2985–2902 Ma; Kositcin and Krapež, 2004; U-Pb detrital zircon SHRIMP). Unconformably overlying the West Rand Group are the quartzite, conglomerate, and shale units of the Central Rand Group (ca. 2902–2849 Ma; Kositcin and Krapež, 2004; U-Pb detrital zircon SHRIMP). The Central Rand Group contains most of the auriferous reefs mined throughout the basin, including the Elsberg, Kloof, Libanon, and Kimberley reefs of the Johannesburg Subgroup, and the Bird, Carbon Leader, North Leader, and Middelvlei reefs of the Turffontein Subgroup (De Kock, 1964). The upper part of the Central Rand Group is unconformably overlain by the VCR of the Venterspost Formation (ca. 2729 ± 19 Ma; Kositcin and Krapež, 2004; U-Pb detrital zircon SHRIMP). The VCR represents an erosional surface that was formed at the end of deposition of the Central Rand Group (McCarthy, 2006).

Above the VCR is the late-Archean Ventersdorp Supergroup (ca. 2.72–2.63 Ga), which comprises ultramafic and mafic lavas of the Klipriviersberg Group (ca. 2709 ± 8 Ma), and metasedimentary rocks and bimodal volcanics of the Platberg Group (Van der Westhuizen et al., 1991). The Pniel Group (Phillips and Law, 2000; Jolley et al., 2004) overlies the Platberg Group and Klipriviersberg Group (cf., Dankert and Hein, 2010).

Unconformably overlying the Ventersdorp Supergroup is the relatively thin Black Reef Formation (BLR), which occurs at the base of the Transvaal Supergroup (ca. 2588 ± 6 Ma; Krapež, 1985; Vos, 1975; Jolly et al., 2004). The Transvaal Supergroup comprises lower and upper successions, namely the Chuniespoort and Pretoria Groups. The dolomites, quartzites, and shales of the Chuniespoort Group were deposited in a stable marine environment, interspersed with lava flows in the upper portion of the stratigraphy (Gibson et al., 2000; McCarthy, 2006).

SEISMIC DATA AND PROCESSING

The merged 2003 Kloof-South Deep, 1988 South Deep, and 1994 Leeudoorn 3D seismic data sets were passed through the same standard workflow, including field preprocessing and full processing. Field processing, which provides brute stacks with elevation corrections, was done to evaluate the quality of the data, estimate the signal-to-noise ratio (S/N), and detect and remove bad and noisy traces. Full processing improved the S/N through various prestack operations such as trace editing, gain recovery, linear noise removal, surface-consistent "spiking" deconvolution, zero phase spectral whitening, trace balancing, velocity picking, and a 35% stretch mute. Appropriate static and phase corrections were calculated and applied prestack before merging the two data sets. A 90° phase shift and −8 ms bulk time shift was applied to the Leeudoorn data to correct for relative phase and time shifts observed between the Kloof-South Deep and Leeudoorn data sets. These two data sets were then successfully merged into one seamless data cube. No evidence of the data merge was identified in the data volume during subsequent analysis and processing.

Subsequent processing steps on the merged cube included the application of refraction statics, normal move-out correction, 3D Kirchhoff dip move-out correction, stacking, final datum shift to 1500 m above sea level, 3D finite difference depth migration, velocity analysis, and prestack time migration (PSTM) using the 3D Kirchhoff algorithm. Finally, depth conversion was carried out using interval velocities derived from surface borehole intersections and PSTM picks of the VCR and BLR. The PSTM depth-domain volume was shifted 330 m to correspond with the 1995 WUDLs datum of 1830 m above the sea level. The WUDLs and the Kloof-South Deep data sets were then merged to produce a single cube. However, the splice between the WUDLs-Driefontein and Kloof-South Deep data is obvious as the 1995 WUDLs-Driefontein data has a lower S/N than the 2003 Kloof-South Deep data.

All seismic data sets contain noise. This noise could result from acquisition, processing artifacts, or random sources. The relatively poor quality of the 1994 Leeudoorn and 1995 WUDLs-Driefontein data sets resulted from the combination of old acquisition systems and processing algorithms. The 1994 Leeudoorn data was reprocessed using PSTM in an attempt to improve the data quality. PSTM is a process by which each trace is migrated before stacking the common offset gathers, and is a relatively advanced migration technique commonly used in the petroleum industry (Yilmaz et al., 2001; Cameron et al., 2008). Prior to the Kloof-South Deep survey, PSTM had not been applied to Witwatersrand Basin data. The technique, generally known to be useful in defining stratigraphic and structural discontinuities in areas characterized by complex faulting and moderate lateral velocity variations, was deemed appropriate for application to the Witwatersrand basin. The application of 3D prestack Kirchhoff time migration to 1994 Leeudoorn data improved imaging of the VCR, faults, and stratigraphy when compared to the older poststack finite difference depth migration technique originally applied to the same data (Figures 3a–3d)

Although PSTM improved the S/N, it should be noted that the northern part of the survey area, accounting for about 5%–8% of the total planned subsurface imaging area, remained poorly imaged due to dolomite outcrops (Figure 4). The deterioration of the seismic data quality over dolomite is a well-known problem (cf., Wright et al., 2000; Šumanovac and Weisser, 2001) not only in South Africa, but elsewhere in the world. The deterioration is the result of scattering of the seismic energy due to karst weathering. It is very unlikely that imaging of the VCR and structures will ever be achieved in this area.

SEISMIC INTERPRETATION METHOD

The interpretation of seismic data was carried out using various advanced seismic interpretation software packages. These packages provide a true 3D modeling and visualization environment, allowing complex geologic modeling of seismic interpretation data, as well as enhanced visualization of faults and horizons.

The seismic reflectors, faults, and other discontinuities were manually picked from trace to trace along inline, crossline, and depth slices. The reliability with which seismic reflectors are picked is a combination of the S/N and structural complexity. Therefore, in structurally complex areas of the study and those zones of data with poor S/N, careful picking of reflections and faults was required before they could be confidently assigned as robust picks in the final geologic model. To map the major structures, seismic sections were initially interpreted at a relatively wide line spacing; for example, every fifth crossline and inline of the seismic volume. Once a wide grid of picks was completed, infill picks were made at a close line spacing, facilitating a detailed structural interpretation. To make sure that subtle faults were not missed during the picking process, every single seismic line was interpreted. Finally, the seismically

Downloaded 09 Sep 2012 to 41.132.206.56. Redistribution subject to SEG license or copyright; see Terms of Use at http://segdl.org/

defined VCR and associated faults were integrated with borehole information to create a robust geologic model of the VCR orebody.

Interpretations of the auriferous VCR and BLR were of particular interest in this study, because the reefs are economically important. The VCR unconformity is a major economic horizon of interest in the Witwatersrand Basin and it forms an important marker across the study area. The depth of the VCR unconformity in the study area is between 2000 and 4500 m below the surface. The VCR is typically less than 2 m thick and is not directly imaged seismically. It occurs at a major and laterally extensive acoustic impedance contrast between high-velocity, dense andesitic lavas of the Klipriviersberg Group and the underlying relatively low-velocity, less-dense quartzite units of the Central Rand Group; i.e., it is the reflective interface that is imaged. Based on interval velocities, the VCR was picked as a peak because of the decrease of seismic velocity from the overlying Ventersdorp Group lavas (approximately 6400 m/s) to the underlying Central Rand quartzite units (approximately 5750 m/s). The interpretation of the VCR surface constrained pre-, syn-, and post-Central Rand Group age structures with a view to developing an understanding of the prevailing tectonic environment.

The quartzites and conglomerates of the BLR produce a prominent and laterally extensive acoustic impedance contrast between the overlying dolomites of the Chuniespoort Group of the Transvaal Supergroup and the underlying lower-velocity, less dense Ventersdorp lavas. This acoustic impedance contrast gives rise to a strong reflection. The BLR was mapped to constrain the ages of structures relative to the deposition of the metasedimentary sequences of the Transvaal Supergroup.

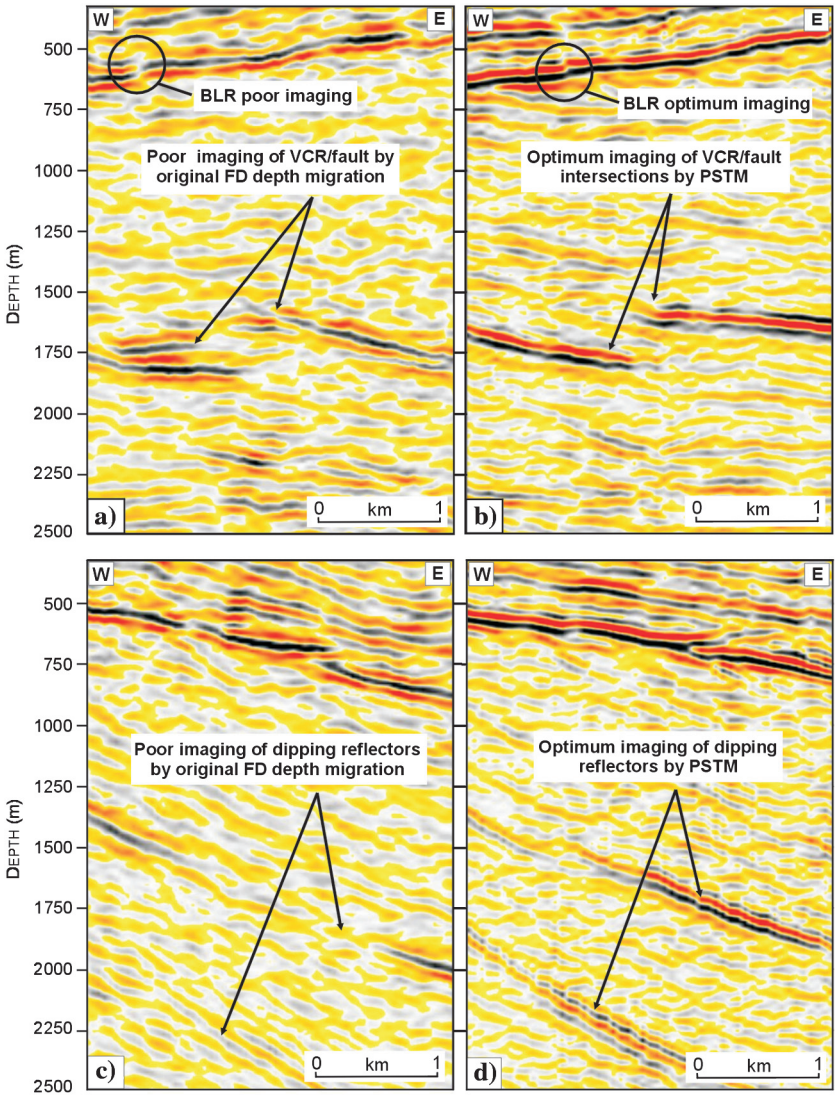

Figure 3. Depth-converted (amplitude display) seismic sections from 1994 Leeudoorn data. (a) The 3D poststack finite difference depth migrated (PSDM) section. (b) The 3D prestack Kirchhoff time migrated (PSTM) section. Note that PSTM shows better resolution relative to the poststack depth migration that was originally applied to the same data set, shown in (a). (c) The 3D poststack depth migrated (PSDM) section. (d) The PSTM section. The PSTM provides better imaging of the dipping reflectors.

SEISMIC RESOLUTION LIMITS AND SEISMIC ATTRIBUTES

The seismic energy is transmitted through the earth as a wave, rather than a narrow beam. Therefore, there is always uncertainty about the exact position of an imaged feature. This uncertainty is often described in terms of the Fresnel Zone. Aspects of the seismic design that were appropriate for assessing the resolution at primary target depths (e.g., VCR at 2000–4500 m) include the dominant frequency (65 Hz), interval velocity (6500 m/s), and dominant wavelength (100 m). Fresnel zone radii of 320 and 475 m were obtained for VCR target depths of 2000 and 4500 m, respectively. A bin size of 25 m was used for stacking, yielding a fold of 32.

Faults with throws that are much less than the dominant seismic wavelength are often difficult to see in the seismic migrated section. Seismic attribute analysis was used to enhance subtle features. Seismic attributes such as dip, azimuth, and edge detection were computed for each horizon to assist the identification of minor faults. The dip and azimuth are the horizon-based seismic attributes most commonly used to enhance structural interpretation (Dalley et al., 1989; Rijks and Jauffred, 1991). The dip and azimuth are, respectively, the magnitude and direction of the gradient vector, which are computed at each grid of the interpreted horizon (Rijks and Jauffred, 1991). The edge detection attributes are a combination of dip and azimuth variations that are normalized to local noise of the interpreted horizon. These attributes are very effective in enhancing structural continuity and detecting crosscutting or conjugate relationships of faults.

RESULTS

At the regional scale, the VCR exhibits a variable strike and dip across the study area as a result of folding, warping, and faulting. The VCR is crosscut by two first-order scale structures, namely, the West Rand and Bank faults, as well

Downloaded 09 Sep 2012 to 41.132.206.56. Redistribution subject to SEG license or copyright; see Terms of Use at http://segdl.org/

as a variety of second and third-order faults. The West Rand and Bank faults generally trend north-northeast and dip to the west (Figures 5 and 6). These faults are listric in form; dipping relatively steeply (65°–70°) at a depth of 1.5 km below the surface, and less steeply (40°) at depths of approximately 3.0–3.5 km below the surface. At greater depths, where the faults intersect the top of the West Rand Group, the dip decreases to 5°–10° before shallowing out within the upper shale units to form a décollement horizon. The West Rand and Bank faults have maximum normal throws of 1.5 and 2.0 km, respectively, and maximum sinistral offsets of 600 and 800 m, respectively (Figures 5 and 6). However, displacement is variable along the strike and dip of the faults, and should be taken into account in mine planning.

Importantly, the West Rand Fault resolves as two sympathetic fault segments that wedge an approximately 100 m wide and 1.0 km long discrete VCR block (Figure 5). The identification of this new VCR block enhances resource calculation and financial valuation of the VCR and life-of-mine planning. The identification

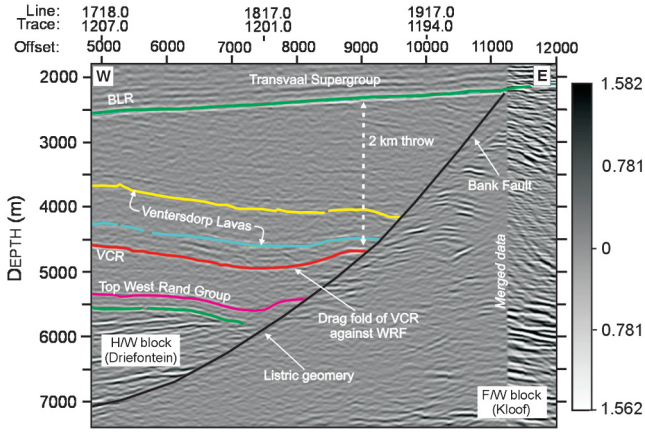

Figure 6. Seismic section (amplitude display) across the Bank Fault with a throw of 2 km showing the listric (concave-up) nature of the fault.

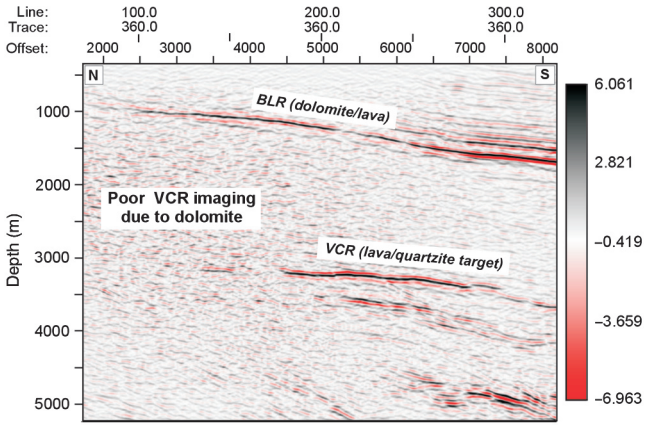

Figure 4. North–south depth–converted PSTM section (amplitude display) clearly showing poor VCR imaging over dolomite outcrop area.

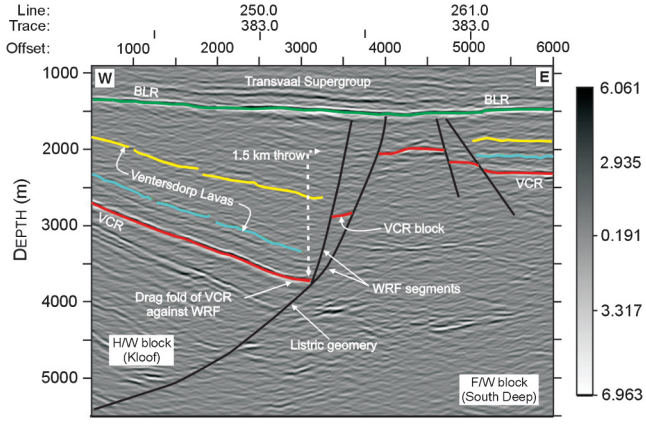

Figure 5. Seismic section (amplitude display) across the West Rand Fault with a throw of 1.5 km in the north of study area, showing sympathetic faults bounding a VCR block in the fault zone.

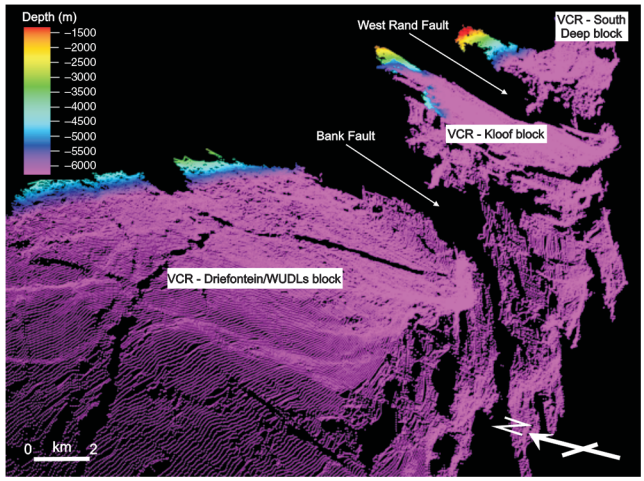

Figure 7. The 3D regional seismic VCR orebody model, with the West Rand Fault and Bank Fault showing similar geometry. The west–east dimension of the image is 28 km.

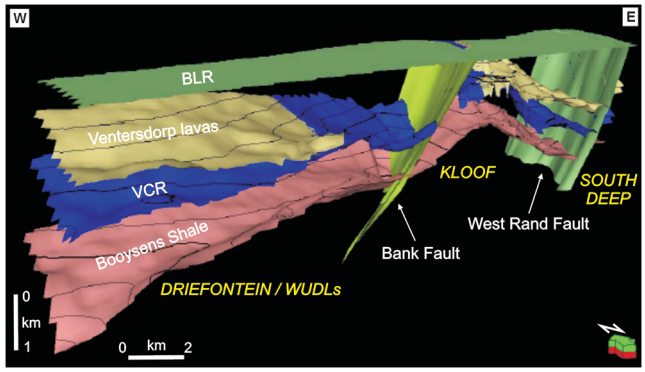

Figure 8. The 3D regional model constructed from reflectors of the BLR, Ventersdorp lavas, VCR, and Booysens Shale.

Downloaded 09 Sep 2012 to 41.132.206.56. Redistribution subject to SEG license or copyright; see Terms of Use at http://segdl.org/

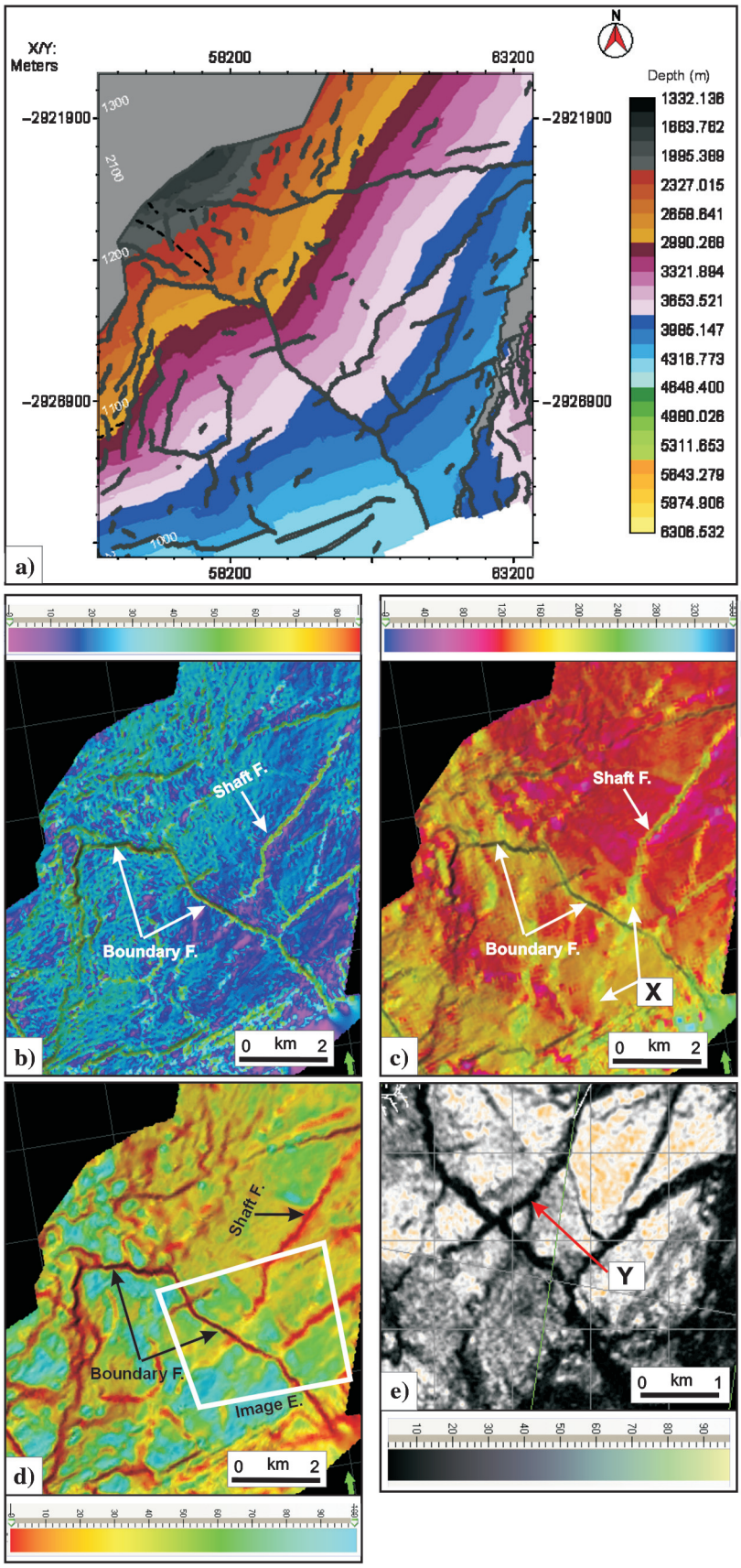

Figure 9. Seismic attributes computed for the VCR horizon at Kloof gold mine. (a) The VCR depth-structure map. (b) Dip attribute display (color bar is given in degrees). (c) Azimuth attribute display, showing the continuation of the shaft fault at position X (color bar is in degrees). (d and e) Color-coded edge attribute displays, clearly showing the crosscutting relationship between the shaft fault and boundary fault (color bar is given in percentages). The SF is seen in image E trending northeasterly; it bifurcates close to the BF (at position Y), and continues on the southwest side of the fault.

Downloaded 09 Sep 2012 to 41.132.206.56. Redistribution subject to SEG license or copyright; see Terms of Use at http://segdl.org/

of the fault-bounded wedge is important for mine planning and safety.

Additionally, several upthrown blocks on the eastern side of the West Rand Fault (Figure 5) that are accessible for mining were also revealed by this study, with considerable gain-of-ground. Thus resource and financial valuation are further enhanced.

In contrast to these discoveries, imaging of the West Rand and Bank faults also indicated they are subtended by clusters of secondary and tertiary faults in their fault damage zones. This is likely to translate into poor ground conditions locally and a loss-of-ground. Clearly, understanding the distribution of the structures is important for (1) predicting face advance rates close to and in fault zones, and (2) wall rock stability around fault zones in terms of fall-of-ground and microseismicity.

Furthermore, the 3D seismic model of the VCR ore horizon (Figure 7) and pre-BLR stratigraphy showed that the West Rand and Bank faults have similar geometries (c.f., Figures 5, 6, 7, and 8); and may have been active at the same time. Importantly, the BLR is not crosscut by major faults in the model, whereas the underlying reflectors are crosscut by faults at all scales. This concurs with studies by Coward et al. (1995), Gibson et al. (2000), Dankert and Hein (2010), and Mambane et al. (2011) which concluded that the West Rand and Bank faults were only active prior to the deposition of the BLR because they do not breach the base of the Transvaal Supergroup. The corollary is that they were excised during a period of significant erosion at the end of deposition of the Pniel Group; i.e., pre-2.58 Ga (cf., Krapež, 1985).

The seismic attributes were able to image faults that are not resolvable using conventional interpretation methods (Figure 9a). The dip and azimuth attributes computed for VCR ore horizon at Kloof survey area successfully imaged smaller faults in the survey area. Comparison of the azimuth and dip attribute maps show that the azimuth attribute map provides a better enhancement of faults relative to dip attribute map (Figure 9b and 9c). For example, the relationship between the northeast-trending Shaft Fault (SF) and northwest-trending Boundary Fault (BF) is well imaged in the azimuth attribute map, but not in the dip attribute map. It is clear that the BF is crosscut by the SF, and is thus older than the SF. This was not known prior to this study. Furthermore, edge detection maps reveal some fault architectures that are not detectable by either conventional picking, the dip, or the azimuth attributes. The SF bifurcates to form a south-southwestern trending branch and a southwest trending branch (Figure 9d and 9e). These structural relationships are difficult to see in seismic sections, and would not have been identified without the application of these attributes. Future mine development plans will need to be updated to take the new structural parameters into account.

Seismic attributes have identified a large number of smaller faults with variable throws that intersect the VCR, some with offsets as small as 15 m or less that would not have been detected through normal picking. Ignorance of these faults could significantly impede mine development, and their heaves (in the case of normal offset) could translate into loss-of-ground and a decrease in the volume of the mineable orebody. However, the attributes failed to identify faults at the edges of the survey where the data were of poor quality. The poor quality of data was an unavoidable effect of the low fold and poor performance of migration near the survey boundaries. It was clear that taking conventionally interpreted ore horizons as true geologic forms leads to a poor model and could increase risk.

The seismic attributes also enhanced 3D accuracy in the positioning of faults that were incorrectly positioned using conventional picking. For example, some of the conventionally picked faults that showed no correlation with VCR topographic breaks were moved to their correct position (Figure 10a and 10b).

The final result of this research has been the development of a regional stratostructural model of the VCR defined from conventional and attribute analysis (Figure 11). The model displays

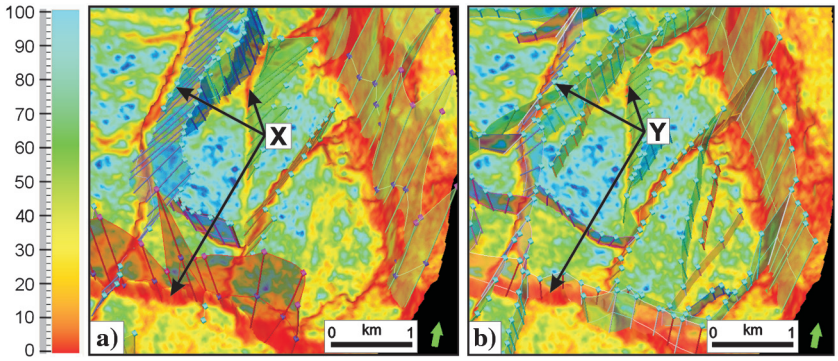

Figure 10. The VCR edge attribute map (color bar is given in percentages). (a) There is a mis-tie between the conventionally picked fault surfaces and the VCR topographic breaks. The position of mis-ties between the VCR breaks and faults is indicated (X). (b) The good tie between fault surfaces and VCR topographic breaks after repositioning of the faults. The positions of good ties between the VCR breaks and faults after modeling is indicated (Y).

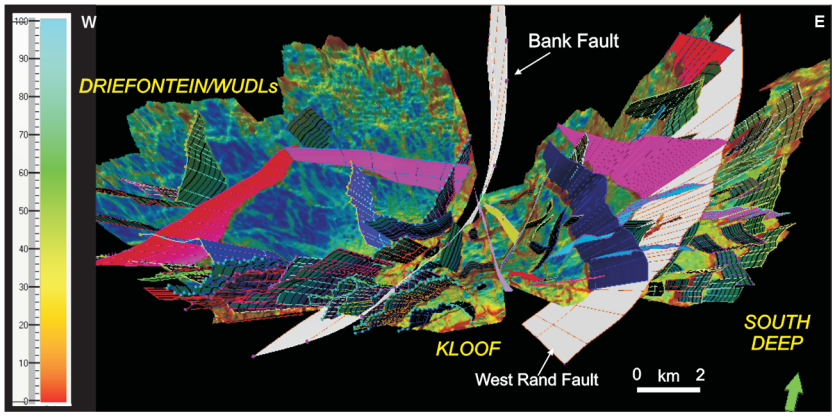

Figure 11. The 3D regional model defined from edge detection attribute analysis constructed from regional VCR pick of the merged surveys (color bar is given in percentages). The model incorporates the major West Rand Fault and Bank Fault, as well as a suite of subtle structures.

Downloaded 09 Sep 2012 to 41.132.206.56. Redistribution subject to SEG license or copyright; see Terms of Use at http://segdl.org/

VCR paleotopography, fault geometries (i.e., dip angles, strike, and dip directions), dikes, and continuity of structures across the mines in the study areas. This model can now be factored into future mine development strategies for better placement of shafts and improved life-of-mine planning; i.e., the high degree of structural resolution afforded by this interpretation will guide future exploration drilling activities and enable the layout of tunnels and stopes to be optimized.

DISCUSSION

With the exception of the unavoidable poor quality of the data in the north of the surveyed area due to outcropping dolomites, the overall quality of the data of the merged 3D seismic reflection surveys was good, providing high-resolution imaging of faults. Further field trials could be conducted in the future to determine parameters that may improve the data in these areas. Parameter testing on a small 2D trial line could investigate (1) increased fold-of-coverage, (2) vibrator force, and (3) an increase in the source effort with longer sweeps.

It is now clear that several structures are laterally continuous across the study area. This understanding could not have been achieved without merging the data sets. The improved acquisition parameters on the 2003 Kloof-South Deep survey, mainly the increased offset, lead to better imaging of the VCR and West Rand Group of reflectors.

Reprocessing of the 1994 Leeudoorn data using PSTM delivered improved VCR and structural imaging; however, the final data are not as good as that of the 2003 Kloof-South Deep surveys. The modeling of first-order structures and their associated second and third-order faults has been possible. The attributes analysis has achieved its objective in reducing structural risk in strategic mine planning. Several structures interpreted by previous workers in noisy areas were found not to exist, whereas many new structures were identified. A structural model incorporating the VCR and faults has been generated for merged data sets, with faults of ~25 m throw being seen, and faults of ~10 m throw being imaged with relative confidence using attribute analysis. The results can be incorporated into geologic plans for each of the mine shafts covered by the surveys.

CONCLUSION

The 3D seismic reflection technique may be deemed very costly. However, its application in the Witwatersrand basin has, over the years, been recognized as a core geophysical method that mitigates the risks associated with the deep mining and drilling of deep costly surface exploration boreholes into faulted areas. The attribute analysis has provided the mines with an improved ability to validate structures, model faults, and their fault loss zones, with throws ranging from 2.5 km, to less than 25 m. By merging the 2003 Kloof-South Deep survey (which incorporated the reprocessed 1994 Leeudoorn survey), and the 1995 WUDLs survey (which incorporated the 1995 Driefontein survey), an extensive and contiguous 3D seismic model of the VCR and BLR has been generated. This model, coupled with the constraining surface borehole data and VCR paleogeomorphological model, will provide Gold Fields Mining Ltd. with a world-class resource model. The seismic model serves as the basis for accurate mine designs and project scheduling.

ACKNOWLEDGMENTS

Gold Fields Mining Ltd. is acknowledged for funding this project and providing permission to publish the results. We wish to thank Schlumberger for providing the Petrel® interpretation software, Rock Deformation Research (RDR), Compagnie Générale de Géophysique (CGG), G. Smith, J. Trickett, L. Lindzay, and M. Muller for their major contribution in this study. Finally, we are also grateful to the SEG associate editors and three anonymous reviewers for their constructive comments and valuable suggestions.

REFERENCES

Cameron, M., S. Fomel, and J. Sethian, 2008, Time-to-depth conversion and seismic velocity estimation using time-migration velocity: Geophysics, **73**, no. 5, VE205–VE210, doi: 10.1190/1.12967501.

Coward, M. P., R. M. Spencer, and C. E. Spencer, 1995, Development of the Witwatersrand Basin, South Africa, *in* M. P. Coward, and A. C. Ries, eds., Early precambrian processes: Geological Society, Special Publications 95, 243–269.

Dalley, R. M., E. C. A. Gevers, G. M. Stampfli, D. J. Davies, C. N. Gastaldi, P. A. Ruijtenberg, and G. J. O. Vermeer, 1989, Dip and azimuth displays for 3D seismic interpretation: First Break, **7**, 86–95.

Dankert, B. T., and K. A. A. Hein, 2010, Evaluating the structural character and tectonic history of the Witwatersrand Basin: Precambrian Research, **177**, 1–22, doi: 10.1016/j.precamres.2009.10.007.

De Kock, M., 1964, The geology and economic significance of the West Wits Line, *in* S. H. Haughton, eds., The geology of some ore deposits in Southern Africa: Geological Society of South Africa, 323–386.

De Wet, J. A. J., and D. A. Hall, 1994, Interpretation of the Oryx 3D seismic survey: Proceedings of the XVth CMMI Congress, South African Institute of Mining and Metallurgy, **3**, 259–270.

Durrheim, R. J., 1986, Recent reflection seismic developments in the Witwatersrand basin, *in* M. Barazangi, and L. Brown, eds., Reflection seismology, a global perspective: American Geophysical Union, Geodynamics Series 13, 77–83.

Gibson, M. A. S., S. J. Jolley, and A. C. Barnicoat, 2000, Interpretation of the Western Ultra Deep Levels 3D seismic survey: The Leading Edge, **19**, 730–735, doi: 10.1190/1.1438704.

Jolley, S. J., S. R. Freeman, A. C. Barnicoat, G. M. Phillips, R. J. Knipe, A. Pather, N. P. C. Fox, D. Strydom, M. T. G. Birch, I. H. C. Henderson, and T. W. Rowland, 2004, Structural controls on Witwatersrand Gold mineralization: Journal of Structural Geology, **26**, 1067–1086, doi: 10.1016/j.jsg.2003.11.011.

Kositcin, N., and B. Krapež, 2004, SHRIMP U-Pb detrital zircon geochronology of the late Archean Witwatersrand Basin, relation between zircon provenance age spectra and basin evolution: Precambrian Research, **129**, 141–168, doi: 10.1016/j.precamres.2003.10.011.

Krapež, B., 1985, The Ventersdorp Contact placer: A gold-pyrite placer of stream and debris-flow origins from the Archaean Witwatersrand Basin of South Africa: Sedimentology, **32**, 223–234, doi: 10.1111/sed.1985.32.issue-2.

Mambane, P. W., K. A. A. Hein, S. G. Twemlow, and M. S. D. Manzi, 2011, Pseudotachylite in the south boundary fault at the Cooke Shaft, Witwatersrand Basin, South Africa: South African Journal of Geology, **114**, 109–120.

McCarthy, T. S., 2006, The Witwatersrand supergroup, *in* M. R. Johnson, C. R. Anhaeusser, and R. J. Thomas, eds., The geology of South Africa: Geological Society of South Africa, Johannesburg/Council for Geosciences, 155–186.

Phillips, G. N., and J. D. Law, 2000, Witwatersrand gold fields: Geology, genesis and exploration, *in* S. G. Hagemann, and P. E. Brown, eds., Gold 2000: Reviews in economic geology, Society for Economic Geology, **13**, 439–500.

Pretorius, C. C., W. H. Steenkamp, and R. G. Smith, 1994, Developments in data acquisition, processing, and interpretation over ten years of south vibroseismic surveying in South Africa: Proceedings of the XVth CMMI Congress, South African Institute of Mining and Metallurgy, **3**, 249–258.

Rijks, E. J. H., and J. C. E. M. Jauffred, 1991, Attribute extraction: An important application in any detailed 3D interpretation study: The Leading Edge, **10**, 11–19.

Stanistreet, I. G., and T. S. McCarthy, 1991, Changing tectonosedimentary: Scenarios relevant to the development of the Late Archaean Witwatersrand Basin: Journal of African Earth Sciences, **13**, 65–81.

Stevenson, F., R. M. A. Higgs, and R. J. Durrheim, 2003, Seismic imaging of precious and base-metal deposits in South Africa, *in* D. W. Eaton, B.

Downloaded 09 Sep 2012 to 41.132.206.56. Redistribution subject to SEG license or copyright; see Terms of Use at http://segdl.org/

Milkereit, and M. H. Salisbury, eds., Hardrock seismic exploration: SEG Geophysical developments, 141–156.
Šumanovac, F., and M. Weisser, 2001, Evaluation of resistivity and seismic methods for hydrogeological mapping karst terrains: Journal of Applied Geophysics, **47**, 13–28, doi: 10.1016/S0926-9851(01)00044-1.
Trickett, J. C., W. A. Duweke, and S. Kock, 2004, Three-dimensional reflection seismic: Worth its weight in platinum: International Platinum Conference, South African Institute of Mining and Metallurgy, 257–264.
Van Der Westhuizen, W. A., H. De Bruiyn, and P. G. Meintjes, 1991, The Ventersdorp supergroup: An overview: Journal of African Earth Sciences, **13**, 83–105.
Vos, R. G., 1975, An alluvial plain and lacustrine model for Precambrian, Witwatersrand Deposits of South Africa: Journal of Sedimentary Petrology, **45**, 480–493.
Weder, E. E. W., 1994, Structure of the area south of the central rand gold mines as derived from a gravity and vibroseis surveys: Proceedings of the XVth CMMI Congress, South African Institute of Mining and metallurgy, 271–281.
Wright, C., E. J. Walls, and D. de J. Carneiro, 2000, The seismic velocity in the vicinity of a mine tunnel at Thabazimbi, South Africa: Journal of Applied Geophysics, **44**, 369–382, doi: 10.1016/S0926-9851(00)00014-8.
Yilmaz, O., I. Tanir, and C. Cregory, 2001, A unified 3D seismic work flow: Geophysics, **66**, 1699–1713, doi: 10.1190/1.1487112.

Downloaded 09 Sep 2012 to 41.132.206.56. Redistribution subject to SEG license or copyright; see Terms of Use at http://segdl.org/